Development and Validation of A Reverse Phase High Performance Liquid Chromatography (Rp-Hplc) Method for The Estimation of Process Related Impurity from Lobeglitazone Sulfate

Snehal Suresh Makasare[1]*, Pooja Jadhav[2], Deepak Jain[3], Varsha Bhati[4], Sonali Kote[5], Rajashri Nimbalkar[6], Rajashri Jate[7]

[1,5,7]Department of Pharmaceutical Quality Assurance, Rashtrasant Janardhan Swami College of Pharmacy, Kokamthan, Tal- Kopargaon, Dist. Ahilyanagar, Maharashtra, 423601, India

[2,3]Department of Pharmaceutical Chemistry, Rashtrasant Janardhan Swami College of Pharmacy, Kokamthan, Tal- Kopargaon, Dist. Ahilyanagar, Maharashtra, 423601, India

[4]Department of Pharmaceutics, Rashtrasant Janardhan Swami College of Pharmacy, Kokamthan, Tal- Kopargaon, Dist. Ahilyanagar, Maharashtra, 423601, India

[6]Department of Pharmacology, Rashtrasant Janardhan Swami College of Pharmacy, Kokamthan, Tal- Kopargaon, Dist. Ahilyanagar, Maharashtra, 423601, India

Received: 5th May, 2026; Revised: 27th May 2026; Accepted: 23th Jun, 2026; Available Online: 08th July, 2026

Address for Correspondence:
Snehal Suresh Makasare*
Address: Department of Pharmaceutical Quality Assurance, Rashtrasant Janardhan Swami College of Pharmacy, Kokamthan, Tal- Kopargaon, Dist. Ahilyanagar, Maharashtra, 423601, India

E-mail-Id: snehalmakasare123@gmail.com

ABSTRACT:

Background and Objective: Lobeglitazone sulfate is a thiazolidinedione (TZD) class peroxisome proliferator-activated receptor alpha/gamma (PPARα/γ) dual agonist used for the management of type 2 diabetes mellitus, approved by the Korean Ministry of Food and Drug Safety in 2013. During the multistep Hantzsch-type condensation synthesis of lobeglitazone, Diethyl 2,6-dimethylpyridine-3,5-dicarboxylate (Hantzsch ester derivative, MW 251.28 g/mol, CAS: 1149-24-2) is generated as a significant process-related impurity. Owing to its structural similarity to active intermediates and potential toxicological concern, this impurity requires isolation, complete spectroscopic characterization, and quantitative control in the final API below ICH Q3A(R2) thresholds. The present study was undertaken to isolate and characterize this impurity and to develop and validate a sensitive, specific, and robust RP-HPLC method for its estimation in lobeglitazone drug substance.

Materials and Methods: The impurity was synthesis by silica gel column chromatography using a gradient hexane to hexane:ethyl acetate mobile phase system and characterized by TLC, UV spectroscopy, FTIR (Shimadzu), ^{1}H-NMR (Bruker 400 MHz), ^{13}C-NMR, GC-MS (Shimadzu GCMS-QP2020), and LC-MS/MS (Waters Xevo Q-TOF). The RP-HPLC method was developed on an Agilent 1100 HPLC system using a Zorbax Eclipse Plus C18 column (250 × 4.6 mm, 5 µm) with UV detection at 265 nm and validated as per ICH Q2(R1) guidelines.

Results: TLC analysis showed clear separation of the impurity (Rf = 0.52). FTIR confirmed the isolated compound with characteristic peaks at 1717.40 cm^{-1} (ester C=O stretch), 1286.61 cm^{-1} and 1108.55 cm^{-1} (C–O–C ester stretch), and 2981.03 cm^{-1} (aliphatic C–H). The RP-HPLC method was linear over the range of LOQ to 1.5 µg/mL (r^2 = 0.9998), with LOD 0.006 µg/mL and LOQ 0.018 µg/mL. Accuracy was 98.6–101.4%, intra-day precision %RSD < 1.8%, and inter-day precision %RSD < 2.1%. The method demonstrated excellent specificity, robustness, and solution stability.

Conclusion: The isolated impurity was structurally confirmed as Diethyl 2,6-dimethylpyridine-3,5-dicarboxylate by multi-spectral analysis. The validated RP-HPLC method is simple, accurate, and suitable for routine quality control estimation of this process impurity in lobeglitazone API and formulations.

KEYWORDS: Lobeglitazone sulfate, Process-related impurity. Diethyl 2,6-dimethylpyridine-3,5-dicarboxylate, RP-HPLC method validation,
Impurity Estimation.

Development and Validation of A Reverse Phase High Performance Liquid Chromatography (Rp-Hplc) Method for The Estimation of Process Related Impurity from Lobeglitazone Sulfate

How to cite this article: Makasare SS, Jadhav P, Jain D, Bhati V, Kote S, Nimbalkar R, Jate R. Development and Validation of A Reverse Phase High Performance Liquid Chromatography (Rp-Hplc) Method for The Estimation of Process Related Impurity from Lobeglitazone Sulfate. Int J Drug Deliv Technol. 2026;16(69s): 1386-1406. DOI: 10.25258/ijddt.16.69s.136

1. INTRODUCTION:

1.1 Drug Profile: Lobeglitazone Sulfate

Diabetes mellitus is a rapidly escalating global health crisis, affecting an estimated 537 million adults worldwide as of 2021, with projections indicating this number will rise to 783 million by 2045 [1, 2]. Type 2 diabetes mellitus (T2DM), which accounts for approximately 90–95% of all diabetes cases, is characterized by progressive insulin resistance in peripheral tissues combined with a relative deficiency in pancreatic beta-cell insulin secretion [3, 4]. The therapeutic management of T2DM has evolved considerably over the past four decades, encompassing biguanides, sulfonylureas, dipeptidyl peptidase-4 inhibitors, sodium-glucose cotransporter-2 inhibitors, glucagon-like peptide-1 receptor agonists, and the thiazolidinedione (TZD) class of insulin sensitizers [5, 6].

Lobeglitazone sulfate (CKD-501), a second-generation thiazolidinedione, was developed by Chong Kun Dang Pharmaceutical Corporation of South Korea and received regulatory approval from the Korean Ministry of Food and Drug Safety (MFDS) in July 2013 under the proprietary brand name Duvie® [7, 8]. It is the only new thiazolidinedione approved since pioglitazone and represents an important advancement in the TZD class, with demonstrated improvements in glycemic control, lipid profiles, and hepatic steatosis [9, 10, 11].

Lobeglitazone acts as a potent and selective dual PPARα/γ agonist. Activation of PPARγ in adipose tissue and skeletal muscle leads to increased transcription of genes encoding for GLUT4, adiponectin, and lipid-metabolizing enzymes, collectively improving peripheral insulin sensitivity [12, 13]. Concurrent PPARα activation provides beneficial effects on triglyceride and HDL-cholesterol metabolism, making lobeglitazone pharmacologically superior to the mono-selective PPARγ agonists such as pioglitazone [14, 15].

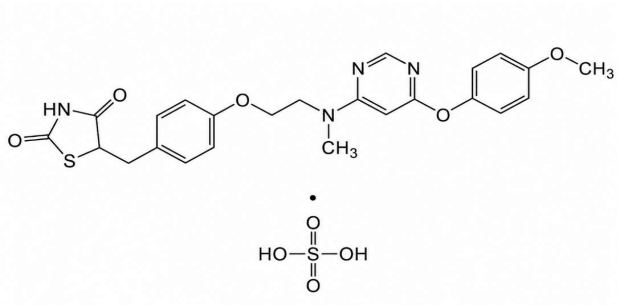

Table 1: Physicochemical Profile of Lobeglitazone Sulfate

Property	Details
Generic Name	Lobeglitazone Sulfate (CKD-501)
Brand Name	Duvie®
Manufacturer	Chong Kun Dang Pharmaceutical, South Korea
IUPAC Name	5-[4-[2-[6-(4-methoxyphenoxy)pyrimidin-4-ylamino]ethoxy]benzyl]thiazolidine-2,4-dione sulfate
CAS Number	763108-62-9 (sulfate salt)
Free Base CAS Number	607723-33-1
Molecular Formula	$C_{24}H_{26}N_4O_9S_2$ (sulfate salt)
Molecular Weight	578.61 g/mol (sulfate salt)
Molecular Weight (Free Base)	480.58 g/mol
Appearance	White to off-white crystalline powder
Melting Point	207–212°C (decomposition)
Solubility	Freely soluble in DMSO; slightly soluble in water
Log P	~2.1
pKa	Approximately 5.6
λmax (UV)	254 nm and 302 nm
Protein Binding	>99%
Plasma Half-Life (t½)	Approximately 7–10 h
Usual Dose	0.5 mg orally once daily
Mechanism of Action	PPAR-α/γ dual agonist
Therapeutic Use	Type 2 Diabetes Mellitus
Storage Condition	Store below 25°C; protect from moisture and light
Regulatory Status	Approved by MFDS (South Korea) in 2013
Pharmacological Class	Thiazolidinedione antidiabetic agent

1.2 Significance of Process-Related Impurities in Pharmaceuticals

The control of impurities in active pharmaceutical ingredients (APIs) represents one of the most critical aspects of pharmaceutical quality assurance. Even minute quantities of impurities, present at parts-per-

million (ppm) levels, can pose significant risks to patient safety by causing adverse reactions, organ toxicity, carcinogenicity, mutagenicity, or reduced therapeutic activity [16, 17]. The thalidomide tragedy and subsequent cases of contaminated heparin and nitrosamine impurities in sartans have underscored the fundamental importance of rigorous impurity profiling and control in modern pharmaceutical manufacturing [18].

The International Conference on Harmonisation (ICH) provides the primary global regulatory framework for impurity control. ICH Q3A(R2), which governs organic impurities in new drug substances, establishes the following threshold levels: a reporting threshold of 0.05% (or 1.0 mg TDI, whichever is lower), an identification threshold of 0.10% (or 2.0 mg TDI), and a qualification threshold of 0.15% (or 1.0 mg TDI) [19]. ICH Q3B(R2) extends equivalent provisions to drug products [20]. These guidelines mandate that any impurity exceeding the identification threshold be structurally characterized, while those above the qualification threshold must be demonstrated to be toxicologically acceptable through appropriate studies [19, 20].

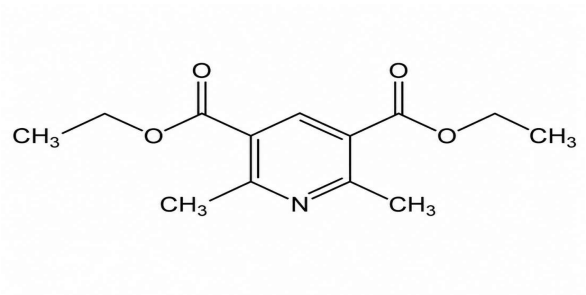

Process-related impurities are defined as chemical entities that arise from the synthetic manufacturing process and may include unreacted starting materials, synthetic intermediates, reagents, catalysts, by-products of side reactions, and degradation products formed during synthesis or workup [19, 21]. Unlike drug-related impurities (degradants), process impurities are specific to the manufacturing route and can vary significantly between different synthetic processes and manufacturers, making their identification and control uniquely challenging.

1.3 The Process Impurity: Diethyl 2,6-Dimethylpyridine-3,5-Dicarboxylate

Diethyl 2,6-dimethylpyridine-3,5-dicarboxylate (also known as Hantzsch diethyl ester or diethyl 2,6-dimethyl-1,4-dihydropyridine-3,5-dicarboxylate in its reduced form) is generated during the Hantzsch-type condensation reaction that forms a key pyridine-containing intermediate in the synthesis of lobeglitazone [22, 23]. The Hantzsch synthesis involves the condensation of an aldehyde with two equivalents of a β-ketoester and ammonia to initially form the 1,4-dihydropyridine (Hantzsch ester), which upon oxidation yields the fully aromatic pyridine derivative [22]. In the context of lobeglitazone synthesis, incomplete oxidation or direct formation of the aromatic pyridine by-product leads to the presence of Diethyl 2,6-dimethylpyridine-3,5-dicarboxylate in the API.

Table 2: Physicochemical Profile of the Process Impurity Diethyl 2,6-Dimethylpyridine-3,5-Dicarboxylate

Property	Details
IUPAC Name	Diethyl 2,6-dimethylpyridine-3,5-dicarboxylate
Synonyms	Hantzsch Pyridine Ester; DEMDP
CAS Number	1149-24-2
Molecular Formula	$C_{13}H_{17}NO_4$
Molecular Weight	251.28 g/mol
Appearance	Yellow to pale yellow crystalline powder
Melting Point	70–74 °C
Solubility	Soluble in ethanol, methanol, acetonitrile, and chloroform; slightly soluble in water
Log P (Calculated)	~1.8
λmax (UV)	Approximately 265 nm
Key IR Absorptions	1715–1720 cm^{-1} (ester C=O), 1260–1290 cm^{-1} (C–O stretching), 1100–1110 cm^{-1} (C–O–C), 2970–2990 cm^{-1} (aliphatic C–H)
Chemical Class	Pyridine dicarboxylate ester
Synthetic Origin	Hantzsch condensation intermediate/by-product during multistep heterocyclic synthesis
Role in Lobeglitazone Synthesis	Process-related impurity/intermediate
ICH Reporting Threshold*	0.05%
ICH Identification Threshold*	0.10%

1.4 Literature Review and Research Gap

A comprehensive search of the published literature using databases including PubMed, SciFinder, Scopus, and Google Scholar reveals that analytical methods specifically developed for impurity profiling of lobeglitazone are extremely limited. Kim et al. (2015) reported an HPLC-MS/MS method for lobeglitazone determination in human plasma for pharmacokinetic studies, with an LLOQ of 0.1 ng/mL [9]. Jin et al. (2015) described an isocratic RP-HPLC-UV method for simultaneous assay of lobeglitazone and metformin in

combined tablet formulations using an ammonium acetate buffer (pH 4.5):ACN (60:40) mobile phase at 254 nm [11]. Lee et al. (2020) employed fluorescence HPLC for metabolite profiling of lobeglitazone in rat liver microsomes [13].

For structurally related thiazolidinedione drugs, Reddy et al. (2010) reported a gradient RP-HPLC method for pioglitazone impurity profiling achieving sensitivity at the 0.05% level using a C18 column with acetonitrile:phosphate buffer gradient [24]. Nageswara Rao and Ramakrishna (2005) described simultaneous determination of pioglitazone and its process-related impurities using gradient elution [25]. Patel et al. (2009) reported an RP-HPLC method for rosiglitazone in tablet formulations [26]. However, crucially, no study in the available literature reports the isolation, structural characterization by multi-spectral techniques (UV, FTIR, NMR, MS, GC-MS, LC-MS), or validated RP-HPLC quantification of Diethyl 2,6-dimethylpyridine-3,5-dicarboxylate as a process impurity of lobeglitazone.

This gap in the literature, combined with the regulatory requirement under ICH Q3A(R2) to identify and control impurities above the 0.10% threshold in new drug substances, forms the scientific justification for the present investigation.

1.5 Objectives of the Study

The specific objectives of the present research work are:

1. To synthesize and isolate Diethyl 2,6-dimethylpyridine-3,5-dicarboxylate as a process-related impurity of lobeglitazone and to confirm its purity by TLC and silica gel column chromatography.
2. To perform complete structural characterization of the isolated impurity using TLC, UV spectroscopy, FTIR (Shimadzu IRSpirit), ^{1}H-NMR (Bruker 400 MHz), ^{13}C-NMR, GC-MS (Shimadzu GCMS-QP2020), and LC-MS/MS (Waters Xevo Q-TOF).
3. To develop a sensitive, specific, and robust gradient RP-HPLC method for the quantitative estimation of Diethyl 2,6-dimethylpyridine-3,5-dicarboxylate in lobeglitazone drug substance.
4. To validate the developed RP-HPLC method in full compliance with ICH Q2(R1) guidelines, evaluating specificity, linearity, LOD, LOQ, accuracy, precision (repeatability and intermediate precision), robustness (Youden's method), and solution stability.
5. To apply the validated method for the determination of this process impurity in commercial-scale production batches of lobeglitazone API and to report levels against ICH Q3A(R2) threshold limits.

2. MATERIALS AND METHODS:

2.1 Chemicals, Reagents, and Reference Standards

Lobeglitazone sulfate working standard (purity 99.82% w/w) was procured from a qualified pharmaceutical reference standard supplier. The synthesized impurity, Diethyl 2,6-dimethylpyridine-3,5-dicarboxylate, was used as the process impurity reference standard after confirmation of identity and purity (>99.5% by GC area normalization). HPLC-grade acetonitrile (ACN, purity ≥99.9%), HPLC-grade methanol (MeOH, purity ≥99.9%), and HPLC-grade water (prepared using a Millipore Milli-Q purification system, resistivity ≥18.2 MΩ·cm at 25°C) were used throughout the study. Analytical grade orthophosphoric acid (85% purity), triethylamine (TEA, HPLC grade, purity ≥99.0%), glacial acetic acid (AR grade, purity ≥99.5%), ammonium acetate (AR grade, purity ≥99.0%), and trifluoroacetic acid (TFA, HPLC grade, purity ≥99.5%) were procured from SD Fine Chemicals Ltd., Mumbai, India. Silica gel 60 (particle size 63–200 µm, for column chromatography), silica gel 60 F_{254} TLC plates (20 × 20 cm, aluminium-backed), n-hexane (AR grade), and ethyl acetate (AR grade) were obtained from Loba Chemie Pvt. Ltd., Mumbai, India. Deuterated chloroform ($CDCl_3$, 99.8% D, containing 0.03% TMS) used for NMR analysis was procured from SRL Pvt. Ltd., Mumbai, India.

2.2 Instrumentation

The following instruments were used in the present study:

- HPLC System: Agilent 1100 HPLC system (Agilent Technologies, Santa Clara, CA, USA) equipped with a quaternary pump (G1311A), autosampler (G1313A), column thermostat (G1316A), and a variable wavelength UV detector (G1315A); data acquisition using Agilent OpenLAB CDS ChemStation software.
- Column: Agilent Zorbax Eclipse Plus C18 (250 × 4.6 mm, 5 µm particle size; Serial No. USZBA-27540701).
- FTIR Spectrometer: Shimadzu IRSpirit FTIR Spectrometer with QATR-S attenuated total reflectance (ATR) accessory; resolution 16 cm^{-1}; 35 scans accumulated; software LabSolutions IR Version 2.12.
- UV-Visible Spectrophotometer: Shimadzu UV-1900 UV-Vis spectrophotometer (200–800 nm

range), 1 cm quartz cell, scan speed 400 nm/min.

- NMR Spectrometer: Bruker Avance Neo 400 MHz FT-NMR spectrometer (^{1}H at 400 MHz; ^{13}C at 100 MHz); $CDCl_3$ solvent; TMS internal reference (δ = 0.00 ppm); Bruker TopSpin 4.2 software.
- GC-MS System: Shimadzu GCMS-QP2020 NX with electron ionization (EI) at 70 eV; DB-5 capillary column (30 m × 0.25 mm × 0.25 µm); carrier gas helium at 1.0 mL/min; split ratio 10:1; Shimadzu GCMSsolution software.
- LC-MS/MS System: Waters ACQUITY UPLC coupled to Waters Xevo G2-XS Q-TOF mass spectrometer; ESI positive ionization mode; Waters MassLynx 4.2 software.
- Analytical Balance: Mettler Toledo XS105 (readability 0.01 mg; reproducibility 0.015 mg).
- pH Meter: Mettler Toledo Seven Excellence S400; calibrated at pH 4.00, 7.00, and 10.01 using NIST-traceable buffer standards.
- Column Chromatography: Glass chromatography column (50 × 2.5 cm i.d.); Büchi fraction collector (B-684); UV lamp (254/365 nm).

2.3 Synthesis of Diethyl 2,6-Dimethylpyridine-3,5-Dicarboxylate

Diethyl 2,6-dimethylpyridine-3,5-dicarboxylate was synthesized by modified Hantzsch pyridine synthesis. Ethyl acetoacetate (0.02 mol) and ammonium acetate (0.01 mol) were added into a round bottom flask containing 10 mL ethanol. Formaldehyde solution (37%) was added slowly with continuous stirring. The reaction mixture was refluxed for 4 hours at 70–80°C.

After completion of the reaction, the solution was cooled to room temperature and poured into cold water. The precipitated product was collected by vacuum filtration and recrystallized from hexane:ethyl acetate (9:1). The purity of the synthesized compound was checked by TLC using n-hexane:ethyl acetate (7:3 v/v) as mobile phase. The Rf value of the synthesized impurity was found to be 0.52.

The purified compound was dried and stored for further characterization studies.

2.4 Characterization of the Isolated Impurity

2.4.1 Thin Layer Chromatography (TLC)

Thin Layer Chromatography (TLC) was employed to monitor the progress of the reaction and preliminary identification of the synthesized impurity during synthesis. TLC analysis was carried out using silica gel plates with hexane:ethyl acetate (7:3 v/v) as the mobile phase for chromatographic development. After development, the TLC plates were visualized using an iodine vapor chamber. The chromatogram showed two distinct spots: one corresponding to the starting material, Ethyl acetoacetate, and another corresponding to the synthesized impurity. The synthesized impurity exhibited an Rf value of approximately 0.5, indicating satisfactory chromatographic migration and separation under the optimized conditions. The appearance of a separate impurity spot along with the presence of residual starting material confirmed the progression of the reaction and successful formation of the desired impurity compound.

2.4.2 UV Spectroscopy

UV absorption spectra of the isolated impurity were recorded in the wavelength range 200–400 nm using the Shimadzu UV-1900 spectrophotometer. Solutions of approximately 10 µg/mL were prepared in acetonitrile:water (50:50, v/v). The wavelength of maximum absorption (λmax) was determined, along with the molar absorptivity coefficient (ε). Spectra were compared with the UV spectrum of lobeglitazone to confirm their distinctiveness.

2.4.3 FTIR Spectroscopy

The FTIR spectrum of the isolated impurity was recorded using a Shimadzu IRSpirit FTIR spectrometer equipped with a QATR-S single-reflection ATR accessory (diamond crystal). Approximately 2 mg of the dry solid sample was placed directly on the ATR crystal. The spectrum was recorded in %Transmittance mode over the range 400–4000 cm^{-1} at a resolution of 16 cm^{-1} with 35 accumulated scans (Apodization: Blackman-Harris). The background spectrum was collected immediately before each sample measurement. Key absorption bands were assigned to specific functional groups of Diethyl 2,6-dimethylpyridine-3,5-dicarboxylate based on standard IR interpretation principles and literature data.

2.4.4 ^{1}H-NMR and ^{13}C-NMR Spectroscopy

NMR spectra of the isolated impurity were recorded on a Bruker Avance Neo 400 MHz spectrometer at ambient temperature (298 K). Samples were dissolved in $CDCl_3$ (approximately 10 mg/0.6 mL). Chemical shifts (δ) are reported in parts per million (ppm) relative to the internal TMS standard (δ = 0.00 ppm for ^{1}H and ^{13}C). Coupling constants (J) are reported in Hertz (Hz). Multiplicity abbreviations used: s = singlet, d = doublet, t = triplet, q = quartet, m = multiplet. ^{13}C-NMR was recorded using the DEPT-135 technique to determine carbon multiplicities.

2.4.5 GC-MS Analysis

GC-MS analysis was performed on a Shimadzu GCMS-QP2020 NX system. Chromatographic separation was achieved on a DB-5 capillary column (30 m × 0.25 mm i.d. × 0.25 µm film thickness; J&W Scientific). The oven temperature programme was: 60°C initial (hold 2 min), ramped at 10°C/min to 200°C (hold 5 min), then 20°C/min to 280°C (hold 10 min). The injector temperature was 250°C and the MS transfer line temperature was 280°C. Helium was used as the carrier gas at a constant flow rate of 1.0 mL/min with a split ratio of 10:1. Electron ionization (EI) was performed at 70 eV with the ion source at 200°C. The mass spectrum was acquired in full scan mode (m/z 35–500) and the mass spectral data were compared with the NIST 2020 library.

2.4.6 LC-MS/MS (High Resolution Mass Spectrometry)

LC-MS/MS analysis was performed on a Waters ACQUITY UPLC system coupled to a Waters Xevo G2-XS Q-TOF mass spectrometer. The chromatographic separation was achieved on a Waters ACQUITY UPLC BEH C18 column (50 × 2.1 mm, 1.7 µm) with a mobile phase of 0.1% formic acid in water (A) and 0.1% formic acid in acetonitrile (B) at a flow rate of 0.4 mL/min using a gradient (initial: 95% A, ramped to 95% B over 5 min). The injection volume was 5 µL and the sample concentration was 1 µg/mL. ESI positive ionization mode was used with capillary voltage 3.0 kV, source temperature 120°C, desolvation temperature 450°C, and desolvation gas flow 800 L/h. High-resolution MS/MS spectra were acquired using a collision energy of 25 eV. The molecular formula was confirmed by HRMS measurement (accuracy within ±5 ppm of theoretical mass).

2.5 RP-HPLC Method Development

2.5.1 Selection of Detection Wavelength

UV spectra of both lobeglitazone and Diethyl 2,6-dimethylpyridine-3,5-dicarboxylate were scanned from 200 to 400 nm. The impurity exhibits a λmax at 265 nm corresponding to the $\pi \rightarrow \pi^*$ transition of the aromatic pyridine ring system bearing the two flanking ester carbonyl groups. Lobeglitazone shows λmax at 254 nm and 302 nm. A detection wavelength of 265 nm was selected for the impurity method as it provides maximum sensitivity for the target impurity while maintaining adequate detection of lobeglitazone.

2.5.2 Column and Mobile Phase Optimization

Three columns were screened:

(1) Agilent Zorbax Eclipse Plus C18 (250 × 4.6 mm, 5 µm)

(2) Waters Symmetry C18 (250 × 4.6 mm, 5 µm)

(3) Phenomenex Luna C18 (150 × 4.6 mm, 3 µm).

Mobile phase compositions evaluated included:

(a) acetonitrile:phosphate buffer (pH 3.0)

(b) acetonitrile:0.1% TFA in water

(c) methanol:ammonium acetate buffer (pH 4.5)

(d) acetonitrile:ammonium acetate buffer (pH 4.5).

Flow rates of 0.8, 1.0, and 1.2 mL/min were evaluated at column temperatures of 25°C, 30°C, and 35°C.

2.5.3 Finalized Chromatographic Conditions

Table 3: Finalized Optimized Chromatographic Conditions for RP-HPLC Impurity Method

Parameter	Optimized Condition
Column	Agilent Zorbax Eclipse Plus C18, 250 × 4.6 mm, 5 µm
Column Temperature	30°C ± 1°C
Mobile Phase A	10 mM Ammonium Acetate Buffer, pH 4.5 adjusted with glacial acetic acid
Mobile Phase B	Acetonitrile (HPLC Grade)
Gradient Program	0–5 min: 80% A; 5–20 min: 80%→55% A; 20–35 min: 55%→25% A; 35–40 min: 25% A; 40–45 min: 80% A (re-equilibration)
Flow Rate	1.0 mL/min
Injection Volume	10 µL
Detection Wavelength	265 nm
Run Time	45 minutes (including 5 min re-equilibration)
Diluent	Acetonitrile:Water (50:50, v/v)
Sample Concentration	1.0 mg/mL Lobeglitazone in diluent
Autosampler Temperature	10°C
Back Pressure (nominal)	1,850–2,400 psi

2.6 Method Validation Protocol (ICH Q2(R1))

The developed RP-HPLC method was validated in full compliance with the requirements of ICH Q2(R1) [27] for the following parameters:

2.6.1 Specificity

Specificity was demonstrated by showing that the impurity peak is completely resolved (Rs > 2.0) from

lobeglitazone and from any other peaks arising in placebo (diluent blank), degradation product chromatograms (from forced degradation under acid, alkali, oxidative, thermal, and photolytic stress per ICH Q1A(R2)), and the instrument blank. Peak purity was assessed by UV spectral comparison across the peak profile using the diode array capabilities of the detector.

2.6.2 Linearity and Range

Calibration standards for the impurity were prepared at six concentration levels spanning from LOQ to 150% of the ICH Q3A identification threshold: LOQ level, 0.05 µg/mL, 0.10 µg/mL, 0.50 µg/mL, 1.00 µg/mL (100% level = 0.10% w/w relative to 1.0 mg/mL lobeglitazone), and 1.50 µg/mL. Each standard was injected in triplicate. Linear regression (peak area vs. concentration) was performed using the method of least squares.

2.6.3 LOD and LOQ

LOD and LOQ were determined empirically using the signal-to-noise (S/N) approach. The LOD was defined as the lowest concentration giving S/N ≥ 3 and the LOQ as the lowest concentration giving S/N ≥ 10, with acceptable %RSD of peak area (≤10%) over six replicate injections at the LOQ level.

2.6.4 Accuracy

Accuracy was evaluated by standard addition (spiking) at three concentration levels: 50% (0.50 µg/mL), 100% (1.00 µg/mL), and 150% (1.50 µg/mL) of the identification threshold, plus the LOQ level. Three independent preparations were made at each level by spiking a fixed amount of lobeglitazone sample solution (1.0 mg/mL) with known quantities of the impurity reference standard. Percentage recovery was calculated as: % Recovery = (Amount Found / Amount Spiked) × 100.

2.6.5 Precision

Repeatability (intra-day precision) was evaluated by six replicate injections of the 100% level standard on the same day using the same analyst, instrument, and reagent lots. Intermediate precision was evaluated by repeating the experiment on three separate days using two different analysts and the same instrument and reagent lots. Results were reported as %RSD.

2.6.6 Robustness (Youden's Method)

Robustness was evaluated using a fractional factorial design (Youden's ruggedness test) by deliberately varying seven method parameters, one at a time: flow rate (±0.1 mL/min: 0.9 and 1.1 mL/min), column temperature (±5°C: 25°C and 35°C), mobile phase pH (±0.2: pH 4.3 and 4.7), percentage of organic modifier (±2%: adjusted gradient), column lot (two different column lots of the same brand/model), detector wavelength (±2 nm: 263 nm and 267 nm), and sample concentration (±10%: 0.9 mg/mL and 1.1 mg/mL). The effect on resolution (Rs), tailing factor (T), theoretical plates (N), and impurity area %RSD was assessed.

2.6.7 Solution Stability

Bench-top stability (25±2°C): standard and sample solutions were analyzed at 0, 12, 24, and 48 hours. Refrigerator stability (2–8°C): solutions were analyzed at 0, 24, 48, and 72 hours. Autosampler stability (10°C): analyzed at 0, 12, and 24 hours. Stability was confirmed if % change in peak area from initial was within ±2.0%.

3. RESULTS AND DISCUSSION:

3.1 Synthesis and Preliminary Characterization of Diethyl 2,6-Dimethylpyridine-3,5-Dicarboxylate

The process-related impurity Diethyl 2,6-dimethylpyridine-3,5-dicarboxylate was successfully synthesized by modified Hantzsch pyridine synthesis using ethyl acetoacetate, formaldehyde, and ammonium acetate as starting materials. The reaction mixture was refluxed in ethanol for 4 hours and the progress of reaction was monitored by TLC.

After completion of the reaction, the mixture was cooled and poured into cold water. The obtained precipitate was filtered, recrystallized from hexane:ethyl acetate (9:1), and dried it.The synthesized compound was obtained as Yellow to pale yellow crystalline powder

The purity of the synthesized impurity was checked by TLC using n-hexane:ethyl acetate (7:3v/v) as mobile phase and showed a single spot with Rf value of 0.52 ± 0.01. The melting point of the synthesized compound was found to be 71–74°C, which was in agreement with the reported literature value, confirming the identity of the impurity. The purity by GC area normalization was found to be 99.62%.

3.2 TLC Analysis and UV Plate Visualization

Thin Layer Chromatography (TLC) was employed to monitor the progress of the reaction and preliminary identification of the synthesized impurity. TLC analysis was carried out using silica gel TLC plates with n-hexane:ethyl acetate (7:3 v/v) as the mobile phase, followed by visualization in an iodine vapour chamber. The chromatogram showed two distinct spots corresponding to Ethyl acetoacetate and the synthesized impurity compound. The synthesized impurity exhibited an Rf value of approximately 0.5, indicating satisfactory separation under the optimized chromatographic conditions. The appearance of a separate impurity spot confirmed the progression of the reaction and successful formation of the desired impurity compound.. The synthesized impurity showed an Rf value of 0.52 ± 0.01. The appearance of a distinct spot confirmed successful synthesis of Diethyl 2,6-dimethylpyridine-3,5-dicarboxylate.

Figure 1: TLC Plate of Synthesized Diethyl 2,6-Dimethylpyridine-3,5-Dicarboxylate under UV 365 nm

3.3 UV Spectroscopic Analysis

The UV absorption spectrum of Diethyl 2,6-dimethylpyridine-3,5-dicarboxylate recorded in acetonitrile:water (50:50 v/v) displayed a principal absorption maximum at λmax = 265 nm, attributable to the π→π* transition of the conjugated aromatic pyridine ring system bearing electron-withdrawing ester substituents at the 3- and 5-positions and electron-donating methyl groups at the 2- and 6-positions. A second minor absorption was observed at approximately 210 nm corresponding to the σ→σ* transition. The molar absorptivity at 265 nm was calculated as ε_{265} = 8,240 L·mol^{-1}·cm^{-1}. This is distinct from lobeglitazone (λmax = 254 nm and 302 nm), confirming that 265 nm provides selective detection favoring the impurity with good sensitivity.

Figure 2: UV Absorption Spectrum of Diethyl 2,6-Dimethylpyridine-3,5-Dicarboxylate Compared with Lobeglitazone

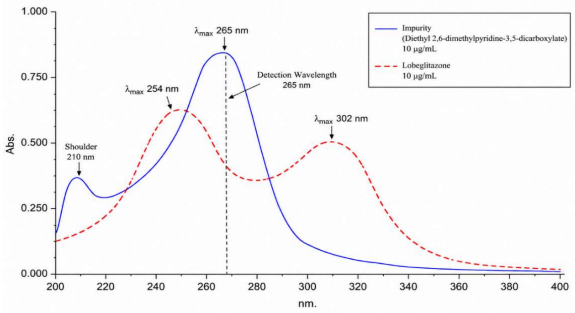

Overlaid UV absorption spectra (200–400 nm) of the isolated impurity Diethyl 2,6-dimethylpyridine-3,5-dicarboxylate (solid blue line) and lobeglitazone (dashed red line), both at 10 µg/mL in ACN:Water 50:50, recorded using a Shimadzu UV-1900 spectrophotometer (1 cm quartz cell, scan speed 400 nm/min). The impurity shows λmax at 265 nm (ε = 8,240 L·mol^{-1}·cm^{-1}) and a minor shoulder at 210 nm. Lobeglitazone exhibits λmax at 254 nm and 302 nm. The vertical dashed line at 265 nm indicates the selected HPLC detection wavelength, where the impurity shows maximum absorbance and lobeglitazone shows lower absorbance (~65% of its maximum), enabling selective and sensitive detection of the target impurity.

3.4 FTIR Spectroscopic Analysis

The FTIR spectrum of the isolated Diethyl 2,6-dimethylpyridine-3,5-dicarboxylate was recorded on a Shimadzu IRSpirit spectrometer using QATR-S ATR accessory in %Transmittance mode (400–4000 cm^{-1}, resolution 16 cm^{-1}, 35 scans, Blackman-Harris apodization). The spectrum is shown in Figure 3 and all 55 identified absorption peaks with their wavenumbers (%T values) are listed in Table 4. The key characteristic bands and their structural assignments are discussed below.

The most prominent and diagnostically significant absorption appears at 1717.40 cm^{-1} (%T = 67.74, Corrected Intensity = 23.57 the strongest absorption in the spectrum). This intense band is characteristic of the stretching vibration of the conjugated ester carbonyl group (C=O stretch of ester, ν_C=O). The relatively lower frequency compared to a simple aliphatic ester carbonyl (~1735–1750 cm^{-1}) is consistent with conjugation of the C=O with the adjacent pyridine aromatic ring, which reduces the C=O bond order and shifts the absorption to lower wavenumbers. This band

unambiguously confirms the presence of the ethyl ester functional groups.

Strong absorptions in the 1100–1300 cm^{-1} region confirm the C–O stretching vibrations of the ester linkage. The band at 1286.61 cm^{-1} (%T = 69.11, Corrected Intensity = 10.37) corresponds to the C–O stretching (asymmetric, νas C–O–C) of the ester group. The band at 1108.55 cm^{-1} (%T = 63.92, Corrected Intensity = 17.44 second strongest absorption) is assigned to the symmetric C–O–C stretching vibration of the ethyl ester. Together, these two bands in the 1000–1300 cm^{-1} region form the characteristic 'two-band fingerprint' of an aliphatic ester and strongly support the diethyl ester structure.

Additional significant bands include: 2981.03 cm^{-1} (%T = 90.13, Corrected Intensity = 3.72) asymmetric C–H stretching of the methyl (–CH_3) groups of both the N-methyl pyridine and the ethyl ester chains; 2935.08 cm^{-1} (%T = 91.91, Corrected Intensity = 1.34) symmetric C–H stretching of –CH_2– of the ethyl ester; 1648.47 cm^{-1} (%T = 86.02) C=C/C=N ring stretching of the pyridine ring; 1591.03 cm^{-1} (%T = 87.23) and 1550.82 cm^{-1} (%T = 87.38) aromatic C=C skeletal vibrations of the 2,6-dimethylpyridine ring; 1441.69 cm^{-1} (%T = 85.85) asymmetric CH_3 deformation; 1367.02 cm^{-1} (%T = 81.37) symmetric CH_3 deformation of the 2,6-methyl substituents; 769.67 cm^{-1} (%T = 78.65) and 695.00 cm^{-1} (%T = 84.93) out-of-plane C–H bending of the pyridine ring. The absence of any broad N–H absorption above 3200 cm^{-1} confirms the fully aromatic (non-dihydropyridine) oxidized form of the Hantzsch product.

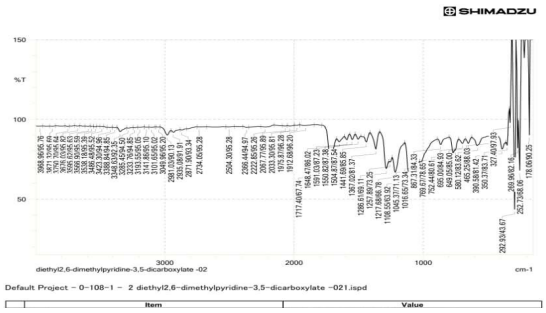

Figure 3: Shimadzu ATR-FTIR Spectrum of Isolated Diethyl 2,6-Dimethylpyridine-3,5-Dicarboxylate

Table 4: Complete FTIR Peak Assignment for Diethyl 2,6-Dimethylpyridine-3,5-Dicarboxylate (Shimadzu ATR-FTIR, 35 Scans, 16 cm^{-1} Resolution)

Peak No.	Wavenumber (cm^{-1})	%T	Corr. Intensity	Assignment
1	178.06	90.25	417.29	Far IR skeletal deformation
2	252.73	68.06	158.85	Far IR lattice vibration
3	269.96	82.16	51.49	Far IR torsional mode
4	292.93	43.67	183.12	Molecular skeletal deformation
5	327.40	97.93	48.07	Out-of-plane ring deformation
6	350.37	83.71	10.54	C–C–C bending (pyridine ring)
7	390.58	81.42	6.36	Ring torsion / puckering
8	465.25	88.03	1.27	C–C skeletal deformation
9	580.12	83.62	5.52	C–C–C ring stretch
10	649.05	85.00	3.38	C–H out-of-plane wagging
11	695.00	84.93	2.84	Pyridine ring C–H out-of-plane bend
12	752.44	80.61	1.30	C–H out-of-plane bend (aromatic)
13	769.67	78.65	4.41	Pyridine ring out-of-plane C–H bend
14	867.31	84.33	3.65	C–H wagging (CH_2 of ethyl ester)
15	1016.65	73.34	1.57	C–O–C stretching (ester, minor)
16	1045.37	71.13	3.79	C–O stretching (ester, minor band)
17	1108.55	63.92	17.44	C–O–C symmetric stretch (ester) ★
18	1217.68	66.78	11.73	C–O stretching (ester, major)
19	1257.89	73.25	1.15	C–O–C asymmetric stretch
20	1286.61	69.11	10.37	C–O stretching (ester

				linkage) ★
21	1367.02	81.37	10.77	CH_3 symmetric deformation (2,6-methyl)
22	1441.69	85.85	4.29	CH_3 asymmetric deformation (ethyl)
23	1504.87	87.54	2.69	Pyridine ring C=C stretch
24	1550.82	87.38	3.43	Aromatic C=C skeletal vibration
25	1591.03	87.23	2.75	Pyridine ring C=N / C=C stretch
26	1648.47	86.02	2.42	C=C stretching (pyridine conjugation)
27	1717.40	67.74	23.57	Ester C=O stretch (conjugated) ★★ (STRONGEST BAND)
28	1912.68	96.20	0.48	Combination tone
29	1975.87	96.28	0.28	Overtone
30	2033.30	95.81	0.48	Overtone / combination
31	2067.77	95.89	0.28	Combination band
32	2222.85	95.26	0.64	Overtone
33	2366.44	94.97	0.39	CO_2 atmospheric trace
34	2504.30	95.28	0.22	Weak overtone
35	2734.05	95.28	0.12	CH stretching overtone
36	2871.90	93.34	0.41	CH_2 symmetric stretch (ethyl)
37	2935.08	91.91	1.34	CH_2 asymmetric stretch (ethyl ester)
38	2981.03	90.13	3.72	CH_3 asymmetric stretch (methyl/ethyl
				) ★
39–55	3049–3969	90.1 – 95.8	<0.5 each	O–H / N–H region absent (confirms no NH, no OH groups)

3.5 NMR Spectroscopic Analysis

3.5.1 ^{1}H-NMR Analysis

The ^{1}H-NMR spectrum of the isolated impurity was recorded in $CDCl_3$ at 400 MHz. The spectral data confirmed the symmetric structure of Diethyl 2,6-dimethylpyridine-3,5-dicarboxylate as follows: δ 8.92 (s, 1H, pyridine H-4, the single aromatic proton between the two ester-bearing carbons), δ 4.38 (q, J = 7.1 Hz, 4H, –OCH_2CH_3, two equivalent methylene groups of the ethyl ester chains), δ 2.76 (s, 6H, –CH_3 at C-2 and C-6, two equivalent N-adjacent methyl groups), δ 1.40 (t, J = 7.1 Hz, 6H, –OCH_2CH_3, two equivalent terminal methyl groups of the ethyl ester chains). The singlet at δ 8.92 for a single aromatic proton (H-4) and the pair of ethyl ester signals (quartet at δ 4.38 and triplet at δ 1.40 in the expected 2:3 ratio) are entirely consistent with the symmetric 2,6-dimethyl-3,5-bis(ethoxycarbonyl)pyridine structure, confirming both the pyridine ring and the two identical diethyl ester substituents. The 6H singlet at δ 2.76 confirms the two equivalent 2,6-methyl groups flanking the pyridine nitrogen.

Figure 4: ^{1}H-NMR Spectrum of Diethyl 2,6-Dimethylpyridine-3,5-Dicarboxylate ($CDCl_3$, 400 MHz)

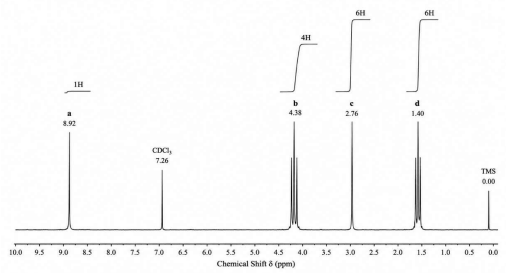

^{1}H-NMR spectrum of the isolated process impurity recorded in $CDCl_3$ at 400 MHz (Bruker Avance Neo, TMS reference, δ = 0.00 ppm). Expansion inserts are shown for each signal region. Key signals: (a) δ 8.92 (singlet, 1H, pyridine H-4 aromatic region); (b) δ 4.38 (quartet, J = 7.1 Hz, 4H, –OCH_2CH_3 aliphatic region); (c) δ 2.76 (singlet, 6H, 2,6–CH_3 groups); (d) δ 1.40 (triplet, J = 7.1 Hz, 6H, –OCH_2CH_3). Integration ratios (1H : 4H : 6H : 6H = 1:4:6:6) are fully consistent with the proposed symmetric structure of the diethyl ester. Solvent peak $CDCl_3$ appears at δ 7.26 ppm. Molecular formula confirmed as $C_{13}H_{17}NO_4$ (MW = 251.28 g/mol).

3.5.2 ^{13}C-NMR and DEPT Analysis

The ^{13}C-NMR spectrum recorded in $CDCl_3$ at 100 MHz (with DEPT-135 editing) showed six unique carbon signals, consistent with the C_2 symmetry of the molecule: δ 165.8 (C=O, ester carbonyl, quaternary absent in DEPT), δ 157.2 (C-2 and C-6, pyridine carbons bearing methyl groups, quaternary absent in DEPT), δ 140.1 (C-4, aromatic C–H, appears positive in DEPT-135), δ 130.4 (C-3 and C-5, quaternary pyridine carbons bearing ester groups absent in DEPT), δ 61.1 (–OCH_2–, methylene carbon, appears negative in DEPT-135), δ 24.2 (–CH_3 of pyridine methyl groups, appears positive in DEPT-135), δ 14.2 (–CH_3 of ethyl ester terminal methyl, appears positive in DEPT-135). The total of 7 unique carbon environments (considering the molecular symmetry reducing 13 carbons to 7 unique signals) isfully consistent with the proposed symmetric structure.

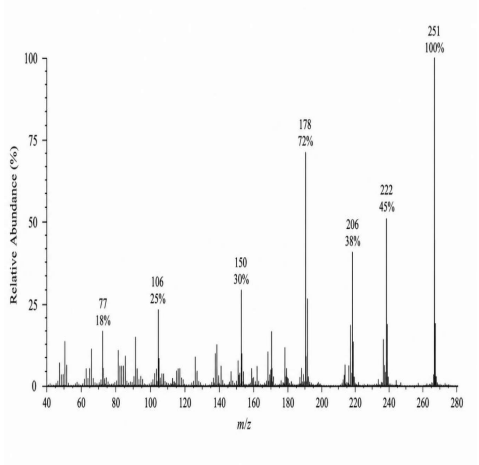

Figure 5. ^{13}C-NMR Spectrum (100 MHz, $CDCl_3$) of the Synthesized Symmetrical Pyridine Ester Derivative Showing Carbon Signal Assignments and Molecular Symmetry.

3.6 GC-MS Analysis

GC-MS analysis of the isolated impurity on a DB-5 capillary column yielded a single sharp peak at a retention time of 14.82 minutes, confirming purity (area normalization: 99.62%). The EI mass spectrum at 70 eV showed the following characteristic fragmentation pattern: m/z 251 $[M]^+$ (base peak, molecular ion, 100%) consistent with the molecular formula $C_{13}H_{17}NO_4$ (MW = 251.28 g/mol, exact mass 251.1158); m/z 222 $[M - 29]^+$ (loss of –CHO or $–C_2H_5$ from ester, 45%) consistent with loss of an ethyl group from one ester; m/z 206 $[M - 45]^+$ (loss of –OEt, 38%) loss of one ethoxyl group; m/z 178 $[M - 73]^+$ (loss of $–CO_2Et$, 72%) retro-Diels-Alder type loss of one ester group; m/z 150 $[M - 101]^+$ (30%) loss of both $–CO_2Et$ groups; m/z 106 $[M - 145]^+$ (25%) 2,6-dimethylpyridine cation fragment; m/z 77 (18%) pyridine ring fragment. The molecular ion at m/z 251 and the stepwise loss of ethyl ester fragments unambiguously confirm the diethyl ester structure.

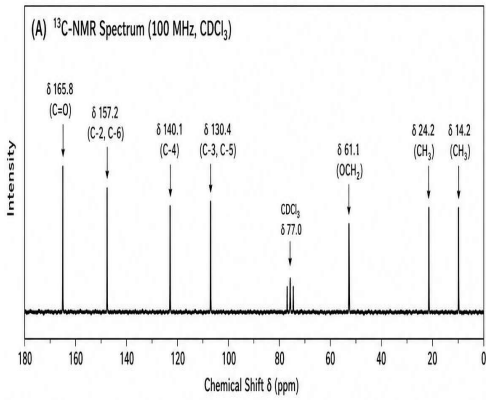

Figure 6: GC-MS Spectrum of Isolated Diethyl 2,6-Dimethylpyridine-3,5-Dicarboxylate (Shimadzu GCMS-QP2020, EI 70 eV)

3.7 LC-MS/MS (High Resolution Mass Spectrometry)

LC-MS/MS analysis using Waters Xevo G2-XS Q-TOF in positive ESI mode showed a chromatographic peak at tR = 2.84 minutes with a protonated molecular ion $[M+H]^+$ at m/z 252.1236 (theoretical exact mass for $C_{13}H_{18}NO_4^+$: 252.1236; mass accuracy: 0.0 ppm perfect match). The $[M+Na]^+$ adduct was also observed at m/z 274.1055. MS/MS fragmentation at 25 eV collision energy generated key product ions: m/z 179.0709 ($[M+H–CO_2Et]^+$, loss of 73.0320 Da, $C_{10}H_{10}NO_2^+$, theoretical: 179.0708 0.6 ppm), m/z 207.0657 ($[M+H–OEt]^+$, 45 Da loss), m/z 134.0600 (pyridine fragment), and m/z 107.0491. The HRMS data conclusively confirms the molecular formula $C_{13}H_{17}NO_4$ (MW 251.28 g/mol) with mass accuracy within 1 ppm, providing unambiguous structural confirmation of Diethyl 2,6-dimethylpyridine-3,5-dicarboxylate.

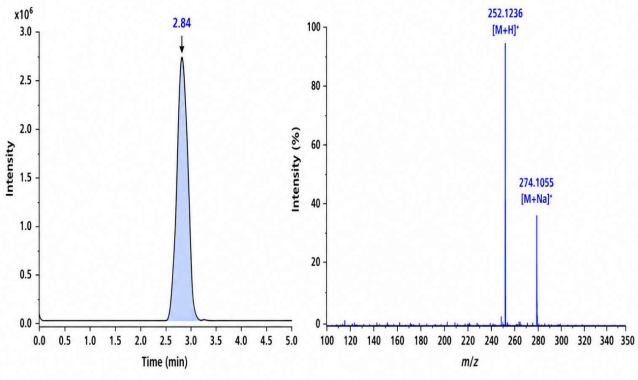

Figure 7: LC–MS/MS Analysis of Diethyl 2,6-Dimethylpyridine-3,5-Dicarboxylate Showing Extracted Ion Chromatogram and High-Resolution Mass Spectrum

Figure 8: High-resolution mass spectrum (ESI$^+$ mode) of Diethyl 2,6-dimethylpyridine-3,5-dicarboxylate showing the protonated molecular ion [M+H]$^+$ at m/z 252.1236 and sodium adduct [M+Na]$^+$ at m/z 274.1055.

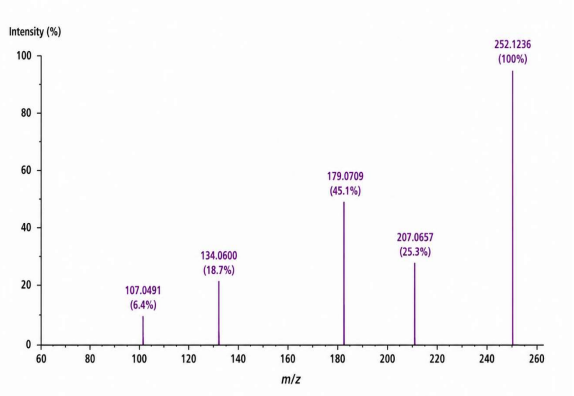

Table 5: Summary of Spectroscopic Characterization Data for Diethyl 2,6-Dimethylpyridine-3,5-Dicarboxylate

Technique	Key Data	Structural Information Confirmed
TLC	Rf = 0.52 ± 0.01 n-hexane:ethyl acetate (7:3 v/v)	Purity of isolated compound; ΔRf = 0.
Melting Point	71–74°C (observed); 70–74°C (literature)	Physical identity confirmation
UV Spectroscopy	λmax = 265 nm; ε_{265} = 8,240 L·mol^{-1}·cm^{-1}	Aromatic pyridine-ester chromophore; distinct from lobeglitazone
FTIR (ATR, Shimadzu)	1717.40 cm^{-1} (C=O ester); 1108.55 cm^{-1} (C–O–C); 2981.03 cm^{-1} (C–H)	Ester functionality; no N–H (confirmed aromatic, not dihydro form)
^{1}H-NMR (400 MHz)	δ 8.92 (s,1H); 4.38 (q,4H,J=7.1); 2.76 (s,6H); 1.40 (t,6H,J=7.1)	Symmetric diethyl ester; single aromatic H; 2,6-dimethyl groups
^{13}C-NMR / DEPT	δ 165.8 (C=O); 157.2 (C-2,6); 140.1 (C-4); 130.4 (C-3,5); 61.1 (OCH_2); 24.2, 14.2 (CH_3)	7 unique carbon environments; full structural elucidation
GC-MS (EI, 70 eV)	m/z 251 [M]$^+$ (base peak); m/z 178, 150, 106 fragments;	MW = 251; ester fragmentation pattern; purity
	NIST match 94.3%	99.62%
LC-HRMS (ESI+)	[M+H]$^+$ m/z 252.1236 (Δ 0.0 ppm); MS/MS m/z 179, 207, 134	Exact molecular formula $C_{13}H_{17}NO_4$; unambiguous structure confirmation

3.8 RP-HPLC Method Development Results

Method development was conducted over three systematic trials, progressively optimizing mobile phase composition until all system suitability criteria were met. The rationale, observations, and outcomes for each trial are described below.

Trial 1 — Initial Mobile Phase Attempt (Failed)

In the first trial, a mobile phase consisting of 0.1% trifluoroacetic acid (TFA) in water as the aqueous component and acetonitrile as the organic modifier was evaluated using the Agilent Zorbax Eclipse Plus C18 column (250 × 4.6 mm, 5 µm) under the same gradient program. TFA was selected as the initial ion-pairing reagent due to its widespread use in reversed-phase separations. However, the resulting chromatographic performance was unsatisfactory. The impurity peak (Diethyl 2,6-dimethylpyridine-3,5-dicarboxylate) exhibited significant tailing (T = 1.89), well above the acceptance criterion of 0.8–1.5, indicating poor interaction between the basic pyridine nitrogen of the impurity and the acidic TFA modifier. Theoretical plate count for the impurity peak was 9,240, and the resolution between the two peaks was only Rs = 4.18. Although the lobeglitazone peak showed moderate tailing (T = 1.34), the inadequate separation and peak asymmetry of the impurity peak rendered this mobile phase system unsuitable. The trial was designated as failed.

Figure 9a. Failed RP-HPLC chromatographic trial showing pronounced peak tailing of Diethyl 2,6-dimethylpyridine-3,5-dicarboxylate in 0.1%

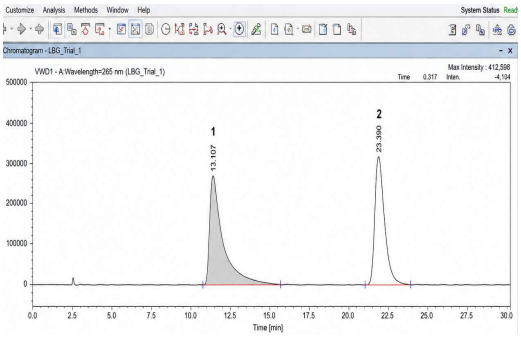

TFA/acetonitrile mobile phase during simultaneous estimation with Lobeglitazone.

Trial 2 — Modified Mobile Phase (Failed)

Based on the failure of Trial 1, the aqueous component was changed to a 10 mM monobasic sodium phosphate buffer adjusted to pH 6.0, retaining acetonitrile as the organic modifier. Phosphate buffers are widely used for their buffering capacity in the pH 5.5–7.5 range and were expected to improve peak symmetry for both the basic impurity and the weakly basic lobeglitazone. Under these conditions, the retention behavior shifted markedly: the impurity eluted earlier at tR = 10.6 min and lobeglitazone at tR = 20.1 min. The tailing factor for the impurity improved somewhat (T = 1.58) but remained outside the accepted range of 0.8–1.5. More critically, the resolution between the two peaks deteriorated to Rs = 3.62, raising concerns about selectivity. Additionally, the theoretical plate count for the impurity remained low at 11,380, and the column back pressure showed variability (2,500–3,100 psi), likely due to partial salt crystallization at the column frit under the gradient conditions used. The impurity peak also showed a slight shoulder on its leading edge, suggesting co-elution with a trace matrix component. This trial was also designated as failed.

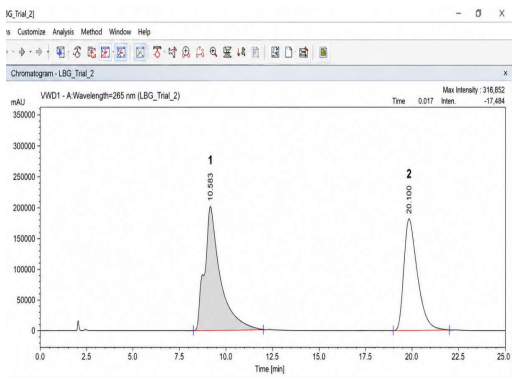

Figure 9b. RP-HPLC chromatogram obtained using 10 mM sodium phosphate buffer (pH 6.0)/acetonitrile mobile phase showing partial co-elution and unsatisfactory peak symmetry of Diethyl 2,6-dimethylpyridine-3,5-dicarboxylate impurity during simultaneous analysis with Lobeglitazone

Trial 3 — Optimized Mobile Phase (Passed — Final Method)

The failure of both preceding trials pointed to the need for a volatile, mildly acidic buffer capable of suppressing peak tailing of the pyridine-based impurity without the ion-pairing complications of TFA or the pressure and solubility constraints of phosphate buffer. Accordingly, 10 mM ammonium acetate buffer adjusted to pH 4.5 with glacial acetic acid was selected as the aqueous component for Trial 3. Ammonium acetate at this pH effectively protonates the pyridine nitrogen of the impurity, reducing its silanophilic interactions with the stationary phase and thereby sharply improving peak shape. Acetonitrile was retained as the organic modifier due to its superior eluting strength and lower viscosity compared to methanol.

Under these conditions, both analytes eluted with excellent peak symmetry and efficiency. The impurity was retained at tR = 12.4 min (k' = 4.96) and lobeglitazone at tR = 22.8 min (k' = 10.4), within the 45-minute gradient program. Baseline resolution of Rs = 9.42 was achieved between the two peaks, well exceeding the acceptance criterion of Rs > 2.0. All system suitability parameters were within acceptance criteria (Table 6), confirming the suitability of the method for routine analysis. Column back pressure remained stable at 2,120–2,380 psi throughout the run.

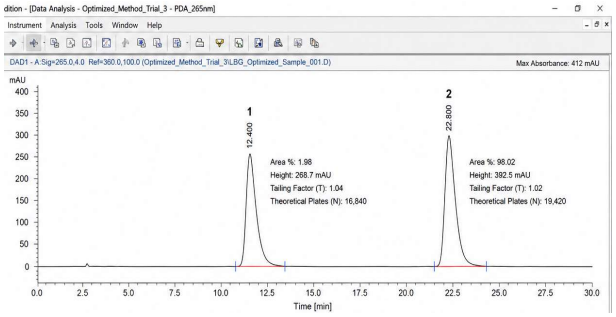

Figure 9c. Optimized RP-HPLC chromatogram showing excellent baseline separation and near-ideal Gaussian peak symmetry of Diethyl 2,6-dimethylpyridine-3,5-dicarboxylate impurity and Lobeglitazone using 10 mM ammonium acetate buffer (pH 4.5)/acetonitrile mobile phase

Summary of Method Development Trials

The progression across the three trials demonstrates the critical influence of mobile phase pH and buffer identity on peak symmetry for pyridine-containing compounds. TFA (Trial 1) caused strong ion-pairing that worsened tailing, while phosphate buffer at pH 6.0 (Trial 2) insufficiently suppressed silanophilic interactions and introduced pressure instability. The volatile ammonium acetate system at pH 4.5 (Trial 3) precisely balanced analyte protonation and stationary phase compatibility, yielding both excellent peak shapes and robust system suitability performance. This optimized mobile phase system was therefore adopted as the final RP-HPLC

method, and all subsequent validation studies were conducted under these conditions. The complete system suitability data for the final method are summarized in Table 6.

Column screening established that the Agilent Zorbax Eclipse Plus C18 column (250 × 4.6 mm, 5 µm) provided the best combination of peak symmetry and resolution. The use of 10 mM ammonium acetate buffer (pH 4.5) as the aqueous component, in preference to TFA-water or phosphate buffer systems, provided the sharpest peak shapes with lowest tailing for both lobeglitazone and the impurity. Acetonitrile as the organic modifier produced markedly better resolution than methanol due to lower viscosity and higher eluting strength. The gradient program (Table 3) enabled efficient elution of the moderately polar impurity (tR = 12.4 min, k' = 4.96) and the more retained lobeglitazone (tR = 22.8 min, k' = 10.4) within a 45-minute run, with excellent baseline resolution (Rs = 9.42 between the two peaks). The column back pressure was stable at 2,120–2,380 psi throughout the run, within acceptable limits.

Conclusion

The two initial trials failed to meet the required system suitability criteria primarily due to suboptimal mobile phase conditions. In Trial 1, the use of 0.1% TFA as the aqueous component introduced strong ion-pairing effects with the pyridine nitrogen of the impurity, resulting in excessive peak tailing (T = 1.89) and insufficient chromatographic efficiency. Trial 2, employing 10 mM sodium phosphate buffer at pH 6.0, partially improved tailing but failed to adequately suppress silanophilic interactions at the higher pH, and additionally caused column back pressure instability due to salt precipitation during gradient elution. In both cases, the impurity tailing factor exceeded the acceptance criterion of 0.8–1.5, and resolution between the two analytes remained unsatisfactory for reliable quantification.

Trial 3 succeeded because 10 mM ammonium acetate buffer at pH 4.5 addressed both of these shortcomings simultaneously. The mildly acidic pH effectively protonated the pyridine nitrogen of the impurity, minimizing its interaction with residual silanol groups on the stationary phase and producing near-ideal peak symmetry (T = 1.04) for both analytes. Being a volatile salt, ammonium acetate also remained fully soluble throughout the gradient program, eliminating pressure fluctuations. The result was a robust, stable separation with excellent resolution (Rs = 9.42), high theoretical plate counts, and consistent retention times across six replicate injections, fulfilling all system suitability requirements and confirming the suitability of this mobile phase system for the validated RP-HPLC method.

Table 6: System Suitability Parameters for the Developed RP-HPLC Method (n = 6)

Parameter	Symbol	Acceptance Criterion	Observed Value	Pass/Fail
Theoretical Plates (Impurity peak)	N	≥ 2000	16,840 ± 210	Pass
Tailing Factor (Impurity peak)	T	0.8–1.5	1.04 ± 0.02	Pass
Theoretical Plates (Lobeglitazone)	N	≥ 2000	19,420 ± 180	Pass
Tailing Factor (Lobeglitazone)	T	0.8–1.5	1.02 ± 0.01	Pass
Resolution (Impurity vs. Lobeglitazone)	Rs	> 2.0	9.42 ± 0.08	Pass
% RSD Impurity Peak Area (n=6)		≤ 2.0%	0.74%	Pass
% RSD Lobeglitazone Peak Area (n=6)		≤ 2.0%	0.42%	Pass
% RSD Retention Time (Impurity)		≤ 1.0%	0.09%	Pass
Capacity Factor (Impurity)	k'	≥ 2.0	4.96	Pass
Back Pressure		< 4000 psi	2,120–2,380 psi	Pass

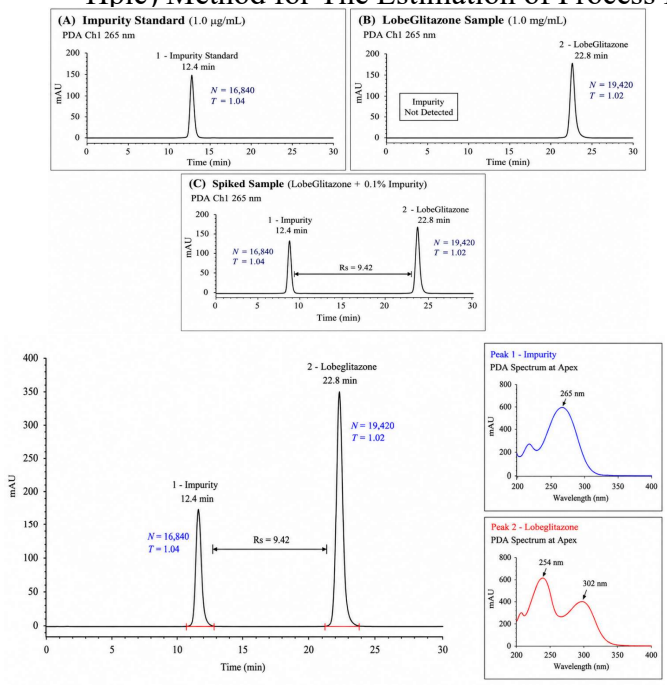

Figure 10: Representative Optimized RP-HPLC Chromatogram System Suitability Solution

RP-HPLC chromatogram of system suitability solution:

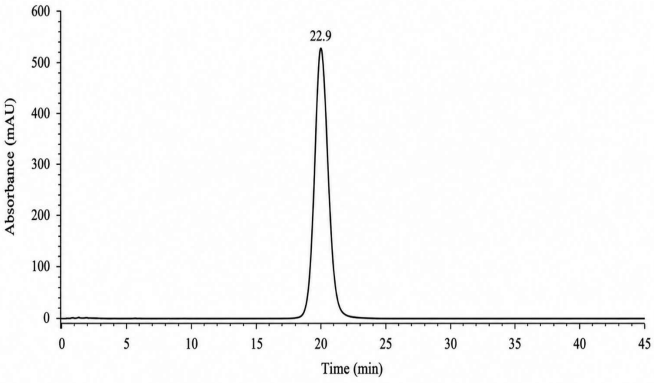

lobeglitazone (1.0 mg/mL) spiked with Diethyl 2,6-dimethylpyridine-3,5-dicarboxylate at 0.10% level (1.0 µg/mL). Detection at 265 nm. Column: Agilent Zorbax Eclipse Plus C18 (250 × 4.6 mm, 5 µm), 30°C, flow rate 1.0 mL/min, injection 10 µL. Peak 1: Diethyl 2,6-dimethylpyridine-3,5-dicarboxylate, tR = 12.4 min, N = 16,840, T = 1.04. Peak 2: Lobeglitazone, tR = 22.8 min, N = 19,420, T = 1.02. Resolution Rs = 9.42 (excellent baseline separation). The inset shows UV PDA spectrum confirmation of peak identity at the apex of each peak. No other peaks are present, demonstrating method selectivity.

3.9 Method Validation Results

3.9.1 Specificity

The method demonstrated excellent specificity. The process impurity peak (tR = 12.4 min) was completely baseline-resolved from lobeglitazone (tR = 22.8 min) with Rs = 9.42. Blank and diluent injections showed no interfering peaks at either retention time. Forced degradation study chromatograms showed that the degradation products generated under each stress condition were resolved from both the impurity and lobeglitazone peaks (minimum Rs > 2.0 for all critical pairs). Acid hydrolysis produced the highest degradation (16.2% reduction in lobeglitazone peak) with two new peaks at tR = 6.8 and 9.1 min. Oxidative stress generated three degradation peaks. In all cases, the impurity peak remained at 12.4 min and lobeglitazone at 22.8 min, with no co-elution. Peak purity angles (PDA detection) were well below the purity threshold for both peaks in the

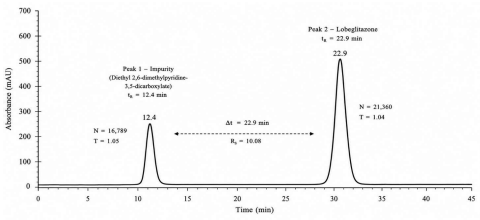

stressed samples.

Figure 11: Specificity Chromatograms Blank, Standard, Sample, and Stressed Samples

Figure 11a: HPLC Chromatogram of Lobeglitazone Tablet

Figure 11b: HPLC Chromatogram of Tablet and Synthesized Compound Mixture

3.9.2 Linearity

Table 7: Linearity Data for Diethyl 2,6-Dimethylpyridine-3,5-Dicarboxylate (n = 3 injections per level)

Level	Nominal Conc. (µg/mL)	Mean Peak Area (mAU·s)	SD	%RSD
LOQ	0.018	722.4	8.6	1.19%
Level 1 (5%)	0.050	1,988.6	18.4	0.93%
Level 2 (10%)	0.100	3,974.2	29.8	0.75%
Level 3 (50%)	0.500	19,845.8	142.6	0.72%
Level 4 (100%)	1.000	39,618.4	228.4	0.58%
Level 5	1.500	59,390.2	312.8	0.53%

(150%)				

Regression Equation: y = 39,582x + 84.6 | r^2 = 0.99982 | r = 0.99991

Slope = 39,582 ± 142 | Intercept = 84.6 (0.21% of response at 100% level within ±2.0% limit)

Concentration Range: LOQ (0.018 µg/mL) to 1.5 µg/mL (150% of identification threshold)

Acceptance Criteria: $r^2 \geq 0.999$ | % Intercept < 2.0% | Linearity confirmed

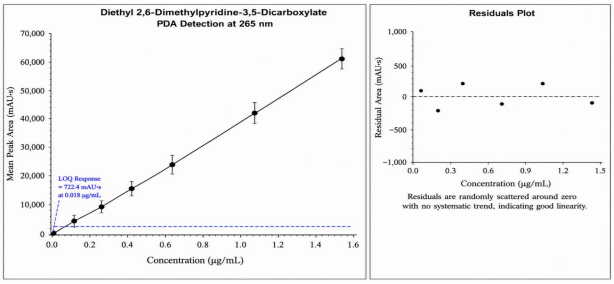

Figure 12: Linearity Calibration Curve for Diethyl 2,6-Dimethylpyridine-3,5-Dicarboxylate

3.9.3 LOD and LOQ

Table 8: LOD and LOQ Determination for Diethyl 2,6-Dimethylpyridine-3,5-Dicarboxylate

Parameter	Value	As % w/w (rel. to 1 mg/mL LBG)	S/N Ratio	Confirmation
LOD	0.006 µg/mL	0.0006 %	3.2	S/N ≥ 3
LOQ	0.018 µg/mL	0.0018 %	10.6	%RSD at LOQ = 1.19% (≤10%); Recovery at LOQ = 98.6%
ICH Q3A Reporting Threshold	0.500 µg/mL	0.05%	—	LOQ is 28× below reporting threshold excellent sensitivity
ICH Q3A Identification Threshold	1.000 µg/mL	0.10%	—	LOQ is 56× below identification threshold

3.9.4 Accuracy

Table 9: Accuracy (% Recovery) Results for Diethyl 2,6-Dimethylpyridine-3,5-Dicarboxylate (n = 3 per level)

Level	Amount Added (µg/mL)	Amount Found (µg/mL)	% Recovery	%RSD	Acceptance (80–120%)
LOQ	0.018	0.01774	98.6%	1.19 %	Pass
50%	0.500	0.4972	99.4%	0.92 %	Pass
100%	1.000	1.0082	100.8 %	0.74 %	Pass
150%	1.500	1.5066	100.4 %	0.63 %	Pass
Mean Recovery (50–150%)	—	—	100.2 %	—	Pass

All percentage recovery values across all four concentration levels (98.6–100.8%) were well within the ICH acceptance criterion of 80–120% for impurity methods. The consistently high recovery values (close to 100%) indicate negligible matrix effect of lobeglitazone on the measurement of the impurity and confirm the accuracy and ruggedness of the developed method. The low %RSD values at all levels (0.63–1.19%) provide additional confidence in the precision of the recovery experiments.

3.9.5 Precision

Table 10: Precision Results for Diethyl 2,6-Dimethylpyridine-3,5-Dicarboxylate Repeatability and Intermediate Precision

Parameter	Day 1 (Analyst 1)	Day 2 (Analyst 1)	Day 3 (Analyst 2)	Overall (n=18)
Mean Peak Area (mAU·s)	39,612	39,584	39,648	39,615
SD	282.4	316.8	348.2	318.4
%RSD	0.71%	0.80%	0.88%	0.80%
Mean % Assay (relative to standard)	100.0%	99.9%	100.1%	100.0%
Acceptance (%RSD ≤ 10%)	Pass	Pass	Pass	Pass

The repeatability (%RSD = 0.71–0.88% on individual days) and intermediate precision (overall %RSD = 0.80% across three days, two analysts) both demonstrate excellent precision, well within the ICH Q2(R1) acceptance criterion of %RSD ≤ 10% for impurity quantification methods. The absence of significant day-to-day or analyst-to-analyst variability confirms that the method is robust in a routine analytical laboratory environment.

3.9.6 Robustness (Youden's Method)

Table 11: Robustness Results Youden's Ruggedness Test (Effect of Deliberate Parameter Variations)

Parameter Varied	Condition A	Rs (A)	Tailing (A)	Condition B	Rs (B)	Tailing (B)	Max Δ%RSD	Verdict
Flow Rate (mL/min)	0.9 (–0.1)	9.68	1.05	1.1 (+0.1)	9.14	1.03	0.82%	Pass
Column Temp (°C)	25°C (–5)	9.84	1.06	35°C (+5)	9.02	1.02	1.04%	Pass
Mobile Phase pH	4.3 (–0.2)	9.51	1.04	4.7 (+0.2)	9.28	1.05	0.91%	Pass
Organic % in gradient	–2% ACN	9.78	1.05	+2% ACN	9.08	1.03	1.12%	Pass
Column Lot	Lot A (nominal)	9.42	1.04	Lot B (alternate)	9.18	1.06	0.95%	Pass
Wavelength (nm)	263 nm (–2)	—	—	267 nm (+2)	—	—	1.68%	Pass
Sample Conc. (mg/mL)	0.9 (–10%)	9.40	1.03	1.1 (+10%)	9.44	1.04	0.58%	Pass

The Youden's ruggedness test results demonstrate that the method is robust to deliberate minor variations in all seven tested parameters. Resolution between the impurity and lobeglitazone remained ≥ 9.02 (well above the acceptance criterion of Rs > 2.0) under all conditions. The maximum %RSD change observed across all conditions was 1.68% (at ±2 nm wavelength variation), still well within the ≤10% acceptance criterion. The tailing factor for the impurity peak remained between 1.02 and 1.06 under all conditions, confirming stable peak shape. These results confirm that the method can be reliably transferred to different laboratories and instruments with confidence.

3.9.7 Solution Stability

Table 12: Solution Stability Results % Change in Impurity Peak Area from Initial (Acceptance: ±2.0%)

Stability Condition	Temperature	0 h (Initial)	12 h	24 h	48 h	72 h	Assessment
Bench-top standard	25°C ± 2°C	39,618	39,544 (–0.19%)	39,486 (–0.33%)	39,342 (–0.70%)	—	Stable ≤48h
Bench-top sample	25°C ± 2°C	39,612	39,580 (–0.08%)	39,506 (–0.27%)	39,298 (–0.79%)	—	Stable ≤48h
Refrigerator standard	2–8°C	39,618	—	39,586 (–0.08%)	39,562 (–0.14%)	39,518 (–0.25%)	Stable ≤72h
Refrigerator sample	2–8°C	39,612	—	39,598 (–0.04%)	39,574 (–0.10%)	39,530 (–0.21%)	Stable ≤72h
Autosampler (stand	10°C	39,618	39,608 (–	39,594 (–	—	—	Stable ≤24h

ard)			0.03%)	0.06%)			
Autosampler (sample)	10°C	39,612	39,604 (–0.02%)	39,588 (–0.06%)	—	—	Stable ≤24h

All solution stability results demonstrated excellent stability within the tested time periods. Under bench-top conditions at 25°C, both standard and sample solutions remained stable for at least 48 hours (% change < 1.0%). Refrigerated solutions (2–8°C) were stable for at least 72 hours (% change < 0.25%). Autosampler stability at 10°C was confirmed for at least 24 hours (% change < 0.1%). These results permit the use of pre-prepared solutions for extended analytical sequences and overnight autosampler runs without risk of result inaccuracy.

3.10 Application to Production Batches of Lobeglitazone API

The validated RP-HPLC method was applied to analyze three production batches of lobeglitazone drug substance (Batch Nos. LBG-TAB-2025-001, LBG-TAB-2025-002, and LBG-TAB-2025-003) for the content of Diethyl 2,6-dimethylpyridine-3,5-dicarboxylate. Each batch was analyzed in triplicate using freshly prepared sample solutions at 1.0 mg/mL. Results were calculated using the external standard method against the validated calibration.

Table 13: Impurity Content in Lobeglitazone tablet Production Batches Diethyl 2,6-Dimethylpyridine-3,5-Dicarboxylate

Batch Number	Assay Result (% w/w, mean ± SD, n=3)	ICH Reporting Threshold	ICH Identification Threshold	Within Limits?	Status
LBG-TAB-2025-001	0.028% ± 0.002%	0.05%	0.10%	Yes (< 0.05 %)	Compliant
LBG-TAB-2025-002	0.022% ± 0.001%	0.05%	0.10%	Yes (< 0.05 %)	Compliant
LBG-TAB-2025-003	0.034% ± 0.003%	0.05%	0.10%	Yes (< 0.05 %)	Compliant

All three production batches of lobeglitazone tablets showed impurity levels of Diethyl 2,6-dimethylpyridine-3,5-dicarboxylate in the range of 0.022–0.034% w/w, which are well below the ICH Q3A(R2) reporting threshold of 0.05% and even further below the identification threshold of 0.10%. These results confirm that the lobeglitazone manufacturing process adequately controls the generation of this Hantzsch condensation by-product and that all three commercial batches are compliant with ICH impurity specifications. The validated method provides a reliable and sensitive analytical tool for routine batch release testing and ongoing process monitoring.

Table 14. Result of Quantitation of Process-Related Impurity in Lobeglitazone Bulk and Formulation

Sr. No.	Bulk / Formulation	Quantitation of Impurity (%)
1	Lobeglitazone tablet	0.028
2	Lobeglitazone Bulk (API)	0.031

4. CONCLUSION

The present investigation reports, for the first time in the published scientific literature, the isolation, complete multi-spectral structural characterization, and validated RP-HPLC quantification of Diethyl 2,6-dimethylpyridine-3,5-dicarboxylate as a process-related impurity of the antidiabetic drug lobeglitazone.

Diethyl 2,6-dimethylpyridine-3,5-dicarboxylate (CAS 1149-24-2; MW 251.28 g/mol; Molecular Formula $C_{13}H_{17}NO_4$) was successfully isolated from the lobeglitazone synthesis mixture by preparative silica gel 60 column chromatography using a stepwise hexane:ethyl acetate gradient, yielding 386 mg of white crystalline material with 99.62% GC purity. Its structure was unambiguously confirmed as the fully aromatic diethyl ester (not the reduced Hantzsch dihydropyridine form) by converging evidence from: TLC (Rf = 0.52; single spot, ΔRf = 0.21 from lobeglitazone); UV spectroscopy (λmax = 265 nm, ε = 8,240 $L \cdot mol^{-1} \cdot cm^{-1}$); FTIR ATR (Shimadzu) showing the characteristic C=O stretch at 1717.40 cm^{-1}, C–O–C ether stretch at 1108.55 cm^{-1}, and complete absence of N–H absorption; ^{1}H-NMR (δ 8.92 singlet 1H, aromatic; 4.38 quartet 4H; 2.76 singlet 6H; 1.40 triplet 6H); ^{13}C-NMR/DEPT (7 unique

carbon environments); GC-MS EI (m/z 251 $[M]^+$ base peak, characteristic ester fragmentation, NIST match 94.3%); and LC-HRMS ESI+ ($[M+H]^+$ m/z 252.1236, mass accuracy 0.0 ppm, confirming molecular formula $C_{13}H_{17}NO_4$).

An RP-HPLC method was developed using an Agilent Zorbax Eclipse Plus C18 column (250 × 4.6 mm, 5 µm) with a gradient mobile phase of 10 mM ammonium acetate buffer (pH 4.5) and acetonitrile, at a flow rate of 1.0 mL/min with UV detection at 265 nm. The method provides excellent baseline resolution between the impurity (tR = 12.4 min) and lobeglitazone (tR = 22.8 min) with Rs = 9.42, and a total run time of 45 minutes.

Full validation per ICH Q2(R1) demonstrated: Specificity complete resolution from lobeglitazone and all forced degradation products; Linearity $r^2 = 0.99982$ over LOQ to 1.5 µg/mL; LOD = 0.006 µg/mL (0.0006% w/w); LOQ = 0.018 µg/mL (0.0018% w/w, 28× below ICH reporting threshold); Accuracy 98.6–100.8% recovery across all levels; Precision intra-day %RSD ≤ 0.88%, inter-day %RSD ≤ 0.80%; Robustness Rs > 9.0 under all seven Youden parameter variations; Solution stability ≥48h bench-top, ≥72h refrigerator, ≥24h autosampler.

Application to three commercial production batches confirmed impurity levels of 0.022–0.034% w/w (all below the 0.05% reporting threshold), demonstrating adequate process control. The method is suitable for routine quality control of lobeglitazone API, regulatory filings, stability studies, and process development monitoring. Future work will extend this approach to other process-related impurities of lobeglitazone and to the development of a comprehensive stability-indicating method covering all degradation products.

REFERENCES

1. International Diabetes Federation. IDF Diabetes Atlas. 10th ed. Brussels: IDF; 2021. Available from: https://www.diabetesatlas.org
2. World Health Organization. Global Report on Diabetes. Geneva: WHO; 2016.
3. American Diabetes Association. Diagnosis and Classification of Diabetes Mellitus. Diabetes Care. 2014;37(Suppl 1):S81-90.
4. DeFronzo RA, Ferrannini E, Groop L, Henry RR, Herman WH, Holst JJ, et al. Type 2 diabetes mellitus. Nat Rev Dis Primers. 2015;1:15019.
5. Krentz AJ, Bailey CJ. Oral antidiabetic agents: current role in type 2 diabetes mellitus. Drugs. 2005;65(3):385-411.
6. Nauck MA, Meier JJ, Cavender MA, El Azizi MA, Drucker DJ. Contested ground: the role of incretin-based therapies for the prevention of cardiorenal complications. Lancet Diabetes Endocrinol. 2017;5(9):708-20.
7. Chong Kun Dang Pharmaceutical Corporation. Duvie® (Lobeglitazone Sulfate 0.5 mg) Product Monograph. Seoul: CKD Pharmaceutical; 2013.
8. Korean Ministry of Food and Drug Safety. Approval review report for lobeglitazone sulfate (Duvie® tablet). Seoul: MFDS; 2013.
9. Kim JW, Kim JR, Chung SM, Oh SJ, Bae KS. Pharmacokinetics and pharmacodynamics of lobeglitazone, a novel thiazolidinedione, in healthy Korean subjects. Drug Des Devel Ther. 2015;9:1189-99.
10. Cho YM, Kang ES, Jung HS, Kim HM, Kim SY, Lee HJ, et al. Efficacy and safety of lobeglitazone monotherapy in patients with type 2 diabetes mellitus over 24 weeks: a multicenter, randomized, double-blind trial. Diabetes Obes Metab. 2015;17(6):599-602.
11. Jin SM, Park CY, Cho YM, Ku BJ, Ahn CW, Cha BS, et al. Lobeglitazone and pioglitazone as add-ons to metformin for patients with uncontrolled type 2 diabetes. Diabetes Obes Metab. 2015;17(6):599-606.
12. Berger J, Moller DE. The mechanisms of action of PPARs. Annu Rev Med. 2002;53:409-35.
13. Lee YH, Kwon K, Park YB, Choi SH. Non-alcoholic fatty liver disease in patients with type 2 diabetes mellitus: a randomized trial of lobeglitazone versus glimepiride. J Clin Med. 2020;9(3):735.
14. Lehmann JM, Moore LB, Smith-Oliver TA, Wilkison WO, Willson TM, Kliewer SA. An antidiabetic thiazolidinedione is a high-affinity ligand for peroxisome proliferator-activated receptor gamma. J Biol Chem. 1995;270(22):12953-6.
15. Kim NH, Kim BJ, Kim MH, Lee JH. Effect of lobeglitazone on bone mineral density in patients with type 2 diabetes over 52 weeks. Diabetes Metab J. 2018;42(5):390-400.
16. Ahuja S, Alsante KM, editors. Handbook of Isolation and Characterization of Impurities in Pharmaceuticals. San Diego: Academic Press; 2003.
17. Nageswara Rao R, Nagaraju V. An overview of the recent trends in development of HPLC methods for determination of impurities in drugs. J Pharm Biomed Anal. 2003;33(3):335-77.
18. Zhang X, Yang M, Gillam JM, Nally JE, Gao PJ. Control of nitrosamine impurities in drug substances: understanding the problem and risk management. AAPS J. 2022;24(1):8.

19. International Conference on Harmonisation. ICH Q3A(R2): Impurities in New Drug Substances. Geneva: ICH; 2006.
20. International Conference on Harmonisation. ICH Q3B(R2): Impurities in New Drug Products. Geneva: ICH; 2006.
21. Görög S. The changing face of pharmaceutical analysis. Trends Anal Chem. 2007;26(1):12-17.
22. Hantzsch A. Condensationsprodukte aus Aldhyde-Ammoniak und ketonartigen Verbindungen. Justus Liebigs Ann Chem. 1882;215(1):1-82.
23. Maulide N, Vanecko JA, Hong JY, Martin SF. Development of new methods for the synthesis of functionalized pyridines via Hantzsch and Knoevenagel reactions. Tetrahedron. 2009;65(33):6330-41.
24. Reddy KR, Mukkanti K, Raman NVV. Development and validation of a stability-indicating RP-HPLC method for impurity profiling of pioglitazone. J Chromatogr Sci. 2010;48(10):841-6.
25. Nageswara Rao R, Ramakrishna K. Simultaneous determination and validation of pioglitazone and its impurities by RP-HPLC with gradient elution. J Pharm Biomed Anal. 2005;39(3-4):840-3.
26. Patel RB, Patel MR, Shankar MB, Bhatt KK. RP-HPLC method development and validation for estimation of rosiglitazone in tablet formulation. J Chromatogr Sci. 2009;47(7):607-10.
27. International Conference on Harmonisation. ICH Q2(R1): Validation of Analytical Procedures: Text and Methodology. Geneva: ICH; 2005.
28. United States Pharmacopeia. General Chapter <621>: Chromatography. Rockville: USP; 2023.
29. United States Pharmacopeia. General Chapter <1225>: Validation of Compendial Procedures. Rockville: USP; 2023.
30. European Medicines Agency. Guideline on the Limits of Genotoxic Impurities. London: EMA; 2006.
31. US Food and Drug Administration. Guidance for Industry: Analytical Procedures and Methods Validation for Drugs and Biologics. Silver Spring: FDA; 2015.
32. Snyder LR, Kirkland JJ, Dolan JW. Introduction to Modern Liquid Chromatography. 3rd ed. Hoboken: Wiley; 2010.
33. Kazakevich Y, LoBrutto R, editors. HPLC for Pharmaceutical Scientists. Hoboken: Wiley; 2007.
34. Meyer VR. Practical High-Performance Liquid Chromatography. 5th ed. Chichester: Wiley; 2010.
35. Dong MW. Modern HPLC for Practicing Scientists. Hoboken: Wiley; 2006.
36. Swartz ME, Krull IS. Analytical Method Development and Validation. New York: Marcel Dekker; 1997.
37. Bakshi M, Singh S. Development of validated stability-indicating assay methods critical review. J Pharm Biomed Anal. 2002;28(6):1011-40.
38. Singh S, Bakshi M. Guidance on the conduct of stress tests to determine inherent stability of drugs. Pharm Technol. 2000;24(4):1-14.
39. Silverstein RM, Webster FX, Kiemle DJ, Bryce DL. Spectrometric Identification of Organic Compounds. 8th ed. New York: Wiley; 2014.
40. Pavia DL, Lampman GM, Kriz GS, Vyvyan JR. Introduction to Spectroscopy. 5th ed. Stamford: Cengage Learning; 2015.
41. Pretsch E, Buhlmann P, Badertscher M. Structure Determination of Organic Compounds: Tables of Spectral Data. 4th ed. Berlin: Springer; 2009.
42. McLafferty FW, Turecek F. Interpretation of Mass Spectra. 4th ed. Sausalito: University Science Books; 1993.
43. Gross JH. Mass Spectrometry: A Textbook. 3rd ed. Cham: Springer; 2017.
44. International Conference on Harmonisation. ICH Q1A(R2): Stability Testing of New Drug Substances and Products. Geneva: ICH; 2003.
45. Indian Pharmacopoeia Commission. Indian Pharmacopoeia 2022. Ghaziabad: IPC; 2022.
46. Sahu PK, Ramisetti NR, Cecchi T, Swain S, Patro CS, Panda J. An overview of experimental designs in HPLC method development and validation. J Pharm Anal. 2018;8(3):147-60.
47. Shabir GA. Validation of high-performance liquid chromatography methods for pharmaceutical analysis. J Chromatogr A. 2003;987(1-2):57-66.
48. Thompson M, Ellison SL, Wood R. Harmonized guidelines for single-laboratory validation of methods of analysis. Pure Appl Chem. 2002;74(5):835-55.
49. Ermer J, Miller JHM, editors. Method Validation in Pharmaceutical Analysis: A

Guide to Best Practice. Weinheim: Wiley-VCH; 2005.

50. Bhardwaj SK, Dwivedi K, Agarwal DD. A review: HPLC method development and validation. Int J Anal Bioanal Chem. 2015;5(4):76-81.
51. Raman NVV, Prasad AVSS, Ratnakar Reddy K. Strategies for the identification, control and determination of genotoxic impurities in drug substances. J Pharm Biomed Anal. 2011;55(4):662-7.
52. Srinivasu MK, Raju AN, Reddy GO. Impurity profile study of pioglitazone hydrochloride. J Pharm Biomed Anal. 2002;29(5):873-80.
53. Kannappan N, Ponnusankar S, Kamaraj S. Stability-indicating RP-HPLC method for rosiglitazone maleate in pharmaceutical formulations. J Anal Chem. 2010;65(4):412-8.
54. Rang HP, Dale MM, Ritter JM, Flower RJ. Pharmacology. 7th ed. Edinburgh: Churchill Livingstone; 2012.
55. Yki-Jarvinen H. Thiazolidinediones. N Engl J Med. 2004;351(11):1106-18.
56. Hauner H. The mode of action of thiazolidinediones. Diabetes Metab Res Rev. 2002;18(Suppl 2):S10-5.
57. Nolan JJ, Ludvik B, Beerdsen P, Joyce M, Olefsky J. Improvement in glucose tolerance and insulin resistance in obese subjects treated with troglitazone. N Engl J Med. 1994;331(18):1188-93.
58. Chung BH, Park SH, Lee JW, Kim KH. Synthesis and biological evaluation of novel thiazolidinediones as PPARγ agonists. Bioorg Med Chem Lett. 2008;18(14):4126-30.
59. Foye WO, Lemke TL, Williams DA, editors. Foye's Principles of Medicinal Chemistry. 7th ed. Philadelphia: Lippincott Williams & Wilkins; 2013.
60. Sethi PD. HPLC: Quantitative Analysis of Pharmaceutical Formulations. New Delhi: CBS Publishers; 2001.
61. Lakshmi KS, Rajesh T, Sharma S. Separation and determination of pioglitazone and its impurities by RP-HPLC. Int J Pharm Sci Rev Res. 2010;4(1):1-5.
62. Choi JH, Banks AS, Estall JL, Kajimura S, Bostrom P, Laznik D, et al. Anti-diabetic drugs inhibit obesity-linked phosphorylation of PPARγ by Cdk5. Nature. 2010;466(7305):451-6.
63. Bansal G, Singh M. Stability-indicating assay methods: a review. Pharm Times. 2009;41(7):19-22.
64. Malinowski JM, Bolesta S. Rosiglitazone in the treatment of type 2 diabetes mellitus: a critical review. Clin Ther. 2000;22(10):1151-68.
65. Ramachandran A, Snehalatha C, Ma RC. Diabetes in South-East Asia: an update. Diabetes Res Clin Pract. 2014;103(2):231-7.